Individual and interactive effects of warming and CO_2 on *Pseudo-nitzschia subcurvata* and *Phaeocystis antarctica*, two dominant phytoplankton from the Ross Sea, Antarctica

Zhi Zhu[1], Pingping Qu[1], Jasmine Gale[1], Feixue Fu[1], David A. Hutchins[1]

1. Department of Biological Science, University of Southern California, Los Angeles, CA 90089, USA.

Correspondence to: David A. Hutchins (dahutch@usc.edu)

Abstract: We investigated the effects of temperature and CO_2 variation on the growth and elemental composition of cultures of the diatom *Pseudo-nitzschia subcurvata* and the prymnesiophyte *Phaeocystis antarctica*, two ecologically dominant phytoplankton species isolated from the Ross Sea, Antarctica. To obtain thermal functional response curves, cultures were grown across a range of temperatures from 0°C to 14°C. In addition, a co-culturing experiment examined the relative abundance of both species at 0°C and 6°C. CO_2 functional response curves were conducted from 100 to 1730 ppm at 2°C and 8°C to test for interactive effects between the two variables. The growth of both phytoplankton was significantly affected by temperature increase, but with different trends. Growth rates of *P. subcurvata* increased with temperature from 0°C to maximum levels at 8°C, while the growth rates of *P. antarctica* only increased from 0°C to 2°C. The maximum thermal limits of *P. subcurvata* and *P. antarctica* where growth stopped completely were 14°C and 10°C, respectively. Although *P. subcurvata* outgrew *P. antarctica* at both temperatures in the co-incubation experiment, this happened much faster at 6°C than at 0°C. For *P. subcurvata*, there was a significant interactive effect in which the warmer temperature decreased the CO_2 half saturation constant for growth, but this was not the case for *P. antarctica*. The growth rates of both species increased with CO_2 increases up to 425 ppm, and in contrast to significant effects of temperature, the effects of CO_2 increase on their elemental composition were minimal. Our results suggest that future warming may be more favorable to the diatom than to the prymnesiophyte, while CO_2 increases may not be a major factor in future competitive interactions between *Pseudo-nitzschia subcurvata* and *Phaeocystis antarctica* in the Ross Sea.

1 Introduction

Global temperature is predicted to increase 2.6°C to 4.8°C by 2100 with increasing anthropogenic CO_2 emissions (IPCC, 2014). The temperature of the Southern Ocean has increased even faster than global average temperature (Meredith and King, 2005), and predicted future climate warming may profoundly change the ocean carbon cycle in this region (Sarmiento et al., 1998). The Ross Sea, Antarctica, is one of the most productive area in the ocean, and features annual austral spring and summer algal blooms dominated by *Phaeocystis* and diatoms that contribute as much as 30% of total primary production in the Southern Ocean (Arrigo et al., 1999, 2008; Smith et al., 2000, 2014a). The responses of phytoplankton in the Ross Sea to future temperature change (Rose et al., 2009; Xu et al., 2014; Zhu et al., 2016) in combination with intensified stratification (Sarmiento et al., 1998) could lead to intensified future diatom blooms (Smith et al. 2014b), and the physiological effects of warming may partially compensate for a lack of iron throughout much of this region (Hutchins and Boyd, 2016).

In the Ross Sea, the colonial prymnesiophyte *Phaeocystis antarctica* typically blooms in austral spring and early summer, and diatoms including *Pseudo-nitzschia subcurvata* and *Chaetoceros* spp. bloom later in the austral summer (Arrigo et al., 1999, 2000; DiTullio and Smith, 1996; Goffart et al., 2000; Rose et al., 2009). Both diatoms and *P. antarctica* play an important role in anthropogenic CO_2 drawdown and the global carbon cycle; additionally, they contribute significantly to the global silicon and sulfur cycles, respectively (Arrigo et al., 1999; Tréguer et al., 1995; Schoemann et al., 2005). Furthermore, the N: P and C: P ratios of *P. antarctica* are higher than those of diatoms, and thus they contribute unequally to the carbon, nitrogen, and phosphorus cycles (Arrigo et al., 1999, 2000). Diatoms are preferred by many planktonic herbivores over *P. antarctica*, and so the two groups also differentially influence the food webs of the Southern Ocean (Knox, 1994; Caron et al., 2000; Haberman et al., 2003).

Arrigo et al. (1999) suggested that the spatial and temporal distributions of *P. antarctica* and diatoms in the Ross Sea are determined by the mixed layer depth, while Liu and Smith (2012) indicated that temperature is more important in shaping the distribution of these two

dominant groups of phytoplankton. Smith and Jones (2015) presented evidence for the importance of deep mixing and the critical depth for the timing of transitions from *P. antarctica* to diatom blooms. Zhu et al. (2016) observed that a 4ºC temperature increase promoted the growth rates of several dominant diatoms isolated from the Ross Sea, including *P. subcurvata*, *Chaetoceros* sp., and *Fragilariopsis cylindrus*, but not the growth rates of *P. antarctica*. In addition, both field and laboratory research has suggested that temperature increase and iron addition can synergistically promote the growth of Ross Sea diatoms (Rose et al., 2009; Zhu et al., 2016; Hutchins and Boyd, 2016). Thus, it is possible that phytoplankton community structure in this region may change in the future under a global warming scenario.

In addition to temperature increases, ocean uptake of 30% of total emitted anthropogenic CO_2 has led to a 0.1 pH unit decrease in surface water, corresponding to a 26% increase in acidity (IPCC, 2014). The global CO_2 concentration is predicted to increase to around 800 ppm by 2100, which will lead to a further decrease in surface seawater pH of 0.3–0.4 units (Orr et al., 2005; IPCC, 2014). CO_2 increases have been found to promote the growth and affect the physiology of many but not all phytoplankton species tested (Fu et al., 2007, 2008; King et al., 2011; Xu et al., 2014; Hutchins and Fu 2017).

Research on the effects of CO_2 increases on *Phaeocystis antarctica* and Antarctic diatoms is still scarce. Xu et al. (2014) suggested that future conditions (higher temperature, CO_2, and irradiance) may shift phytoplankton community structure towards diatoms and away from *P. antarctica* in the Ross Sea. Trimborn et al. (2013) discovered that the growth rates of *P. antarctica* and *P. subcurvata* were not significantly promoted by high CO_2 relative to ambient CO_2 at 3°C. In contrast, Wang et al. (2010) observed that the growth rates of the closely related temperate colonial species *Phaeocystis globosa* increased significantly at 750 ppm CO_2 relative to 380 ppm CO_2.

Many studies have shown that primary production in various parts of the Southern Ocean is limited by iron supply (Martin et al., 1990; Takeda, 1998; Boyd et al., 2000; Sedwick et al., 2000; Hutchins et al., 2002; Coale et al., 2004), and several have addressed the effects of iron

and warming on the growth of phytoplankton from the Ross Sea (Rose et al., 2009; Zhu et al., 2016; Hutchins and Boyd 2016). Thus, an important goal of phytoplankton research is to also gain an understanding of how global warming together with ocean acidification may shift the phytoplankton community in the Ross Sea (Arrigo et al., 1999; DiTullio et al., 2000). This study aimed to explore the effects of increases in temperature and CO_2 availability, both individually and in combination, on *P. antarctica* and *P. subcurvata* isolated from the Ross Sea, Antarctica. These results may shed light on the potential effects of global change on the marine ecosystem and the cycles of carbon and nutrients in the highly productive coastal polynyas of Antarctica.

2 Materials and Methods

2.1 Strains and growth conditions

P. subcurvata and *P. antarctica* were isolated from the ice edge in McMurdo Sound (77.62° S, 165.47° E) in the Ross Sea, Antarctica during January 2015; *P. antarctica* cultures grew as small colonies (~4-12 cells) in all the experiments. All stock cultures were grown in Aquil* medium (100 µmol L^{-1} NO_3^-, 100 µmol L^{-1} SiO_4^{4-},10 µmol L^{-1} PO_4^{3-}) made with 0.2 µM-filtered seawater that was collected from the same Ross Sea locale as the culture isolates (Sunda et al., 2005). Stock and experimental cultures were grown in Fe-replete Aquil medium (0.5 µM). Although phytoplankton in the open Ross Sea polynya are generally proximately iron-limited (Ryan-Keogh et al. 2017), these culture conditions are relevant to the coastal McMurdo Sound ice edge environment in the early spring when Fe is relatively abundant, and typically not limiting. This 'winter reserve' iron is then drawn down in this nearshore environment over the course of the seasonal algal bloom to eventually reach limiting levels (Sedwick et al., 2011; Bertrand et al., 2015). Our experiments address warming and acidification responses in *P. subcurvata* and *P. antarctica* in the absence of any differential effects of Fe availability; interactive effects of Fe limitation with warming and/or acidification in these two species are presented in Xu et al. (2014) and Zhu et al. (2016). Cultures were maintained at 0°C in a walk-in incubator under 24 h cold white fluorescence light (80 µmol photons m^{-2} s^{-1}).

2.2 Experimental design

For thermal functional response curves, experimental cultures of both phytoplankton were grown in triplicate 500 ml acid washed polycarbonate bottles and gradually acclimated by a series of step-wise transfers to a range of temperatures, including 0°C, 2°C, 4°C, 6°C, 8°C, and 10°C (*P. antarctica* died at 10°C) under the same light cycle as stock cultures. Cultures were diluted semi-continuously following Zhu et al. (2016), allowing them to be maintained in continuous exponential growth and so facilitating comparisons between treatments in the same physiological growth stage. All of the cultures were acclimated to their respective temperatures for 8 weeks before the commencement of the experiment. At this point, after the growth rates were verified to be stable for at least three to five consecutive transfers, the cultures were sampled 48 h after dilution (Zhu et al., 2016).

For CO_2 functional response curves, *P. antarctica* and *P. subcurvata* were also grown in triplicate in a series of six CO_2 concentrations from ~100 ppm to ~1730 ppm in triplicate 500 ml acid washed polycarbonate bottles at both 2°C and 8°C using same dilution technique as above. The CO_2 concentration was achieved by gently bubbling with 0.2 μm filtered air/CO_2 mixture (Gilmore, CA) and carbonate system equilibration was ensured by pH and dissolved inorganic carbon (DIC) measurements (King et al., 2015, see below).

An additional experiment tested whether temperature-related trends in growth rates observed in monocultures were maintained when both species were grown together in a simple model community. For this examination of thermal effects on the growth of *P. antarctica* and *P. subcurvata* in co-culture (pre-acclimated to respective temperatures), the isolates were mixed at equal Chl *a* (chlorophyll *a*) concentrations and grown together for 6 days in triplicate bottles at both 0°C and 6°C. These temperatures chosen to span the optimum growth ranges of both species (see Results, below). The relative abundance of each phytoplankton was then calculated based on cell counts taken on days 0, 3 and 6.

2.3 Growth rates

Cell count samples were counted on a Sedgewick Rafter Grid using an Olympus BX51 microscope before and after dilution for each treatment. Samples that couldn't be counted

immediately were preserved with Lugol's (final concentration 2%) and stored at 4°C until counting. Specific growth rates (d^{-1}) were calculated following Eq. (1):

$$\mu = (\ln N_1 - \ln N_0)/t, \quad (1)$$

where N_0 and N_1 are the cell density at the beginning and end of a dilution period, respectively, and t is the duration of the dilution period (Zhu et al. 2016). The Q_{10} of growth rates was calculated following Chaui-Berlinck et al. (2002) as Eq. (2):

$$Q_{10} = (\mu_2/ \mu_1)^{10/(T_2-T_1)}, \quad (2)$$

where μ_1 and μ_2 are the specific growth rates of the phytoplankton at temperatures T_1 and T_2, respectively. The growth rates were fitted to Eq. (3) to estimate the thermal reaction norms of each species:

$$f(T) = ae^{bT}(1- ((T-z)/(w/2))^2), \quad (3)$$

where specific growth rate *f* depends on temperature (T), temperature niche width (*w*), and other empirical parameters *z*, *a*, and *b* were estimated by maximum likelihood (Thomas et al., 2012; Boyd et al., 2013). Afterwards, the optimum temperature for growth and maximum growth rate were estimated by numerically maximizing the equation (Boyd et al., 2013). The growth rates of all the species at all the CO_2 levels were fitted to Michaelis-Menten equation as Eq. (4):

$$\mu = \mu_{max} S/(K_m + S), \quad (4)$$

to estimate maximum growth rates (μ_{max}) and half saturation constants (K_m) for CO_2 concentration (S). In the CO_2 curve experiments growth rates for both these autotrophic species were assumed to be zero at 0 ppm CO_2, and in the thermal curve experiments growth rates were assumed to be zero at -2°C, approximately the freezing point of seawater.

2.4 Elemental and Chl *a* analysis

Culture samples for particulate organic carbon/nitrogen (POC/PON) and particulate organic phosphorus (POP) analyses were filtered onto pre-combusted (500°C for 2 h) GF/F filters and dried at 60°C overnight. A 30 ml aliquot of *P. subcurvata* culture for each treatment were filtered onto 2 μm polycarbonate filters (GE Healthcare, CA) and dried in a 60°C oven overnight for biogenic silica (BSi) analysis. The analysis method of POC/PON and POP

followed Fu et al. (2007), and BSi analysis followed Paasche et al. (1973). An aliquot of 30 to 50 ml from each treatment replicate was filtered onto GF/F filters and extracted with 90% acetone at -20°C for 24 h for Chl *a* analysis. The Chl *a* concentration was then determined using the non-acidification method on a 10-AU^{TM} fluorometer (Turner Design, CA) (Fu et al., 2007).

2.5 pH and dissolved inorganic carbon (DIC) measurements

pH was measured using a pH meter (Thermo Scientific, MA), calibrated with pH 7 and 10 buffer solutions. For DIC analyses, an aliquot of 25 mL was preserved with 200 µL 5% $HgCl_2$ and stored in the dark at 4°C until analysis. Total DIC was measured using a CM140 Total Inorganic Carbon Analyzer (UIC Inc., IL). An aliquot of 5 mL sample was injected into the sparging column of Acidification Unit CM5230 (UIC Inc., IL) followed by 2 ml 10% phosphoric acid. By using flow rates controlled pure nitrogen as carrier gas, and the CO_2 released from the DIC pool in the sample was quantified with a CM5015 CO_2 Coulometer (UIC Inc., IL) using absolute coulometric titration. The carbonate buffer system was sampled for each of the triplicate bottles in each treatment at the beginning and end of the experiments; reported values are final ones. The pCO_2 in growth media was calculated using CO2SYS (Pierrot et al., 2006). These carbonate system measurements are shown in Table 1, along with the corresponding calculated pCO_2 values calculated. Kinetic parameters were calculated using the individual calculated pCO_2 values for each replicate (see above), but for convenience, the CO_2 treatments are referred to in the text using the mean value of all experimental bottles, rounded to the nearest 5 ppm: these values are 100 ppm, 205 ppm, 260 ppm, 425 ppm, 755 ppm, and 1730 ppm.

2.6 Statistical analysis

All statistical analyses and model fitting, including student t-tests, ANOVA, Tukey's HSD test, two-way ANOVA, and thermal reaction norms estimation were conducted using the open source statistical software R version 3.1.2 (R Foundation).

3 Results

3.1 Temperature effects on growth rates

Temperature increase significantly affected the growth rates of both *P. antarctica* and *P. subcurvata*, but with different trends ($p < 0.05$) (Fig. 1). The specific growth rates of *P. subcurvata* increased from 0°C to 8°C ($p < 0.05$), and then significantly decreased at 10°C ($p < 0.05$) (Fig. 1). The growth rates of *P. antarctica* significantly increased from 0°C to 2°C, and plateaued at 4°C and 6°C, and then significantly decreased from 6°C to 8°C ($p < 0.05$) (Fig. 1). *P. antarctica* and *P. subcurvata* stopped growing at 10°C and 14°C, respectively (Fig. 1A). The specific growth rates of *P. subcurvata* were not significantly different from those of *P. antarctica* at 0°C, 2°C and 4°C, but became significantly higher than *P. antarctica* at 6°C, and remained significantly higher than *P. antarctica* through 8°C and 10°C ($p < 0.05$) (Fig. 1A). The optimum temperatures for growth of *P. antarctica* and *P. subcurvata* were 4.85°C and 7.36°C, respectively, both well above the current temperature in the Ross Sea, Antarctica (Table 2). In addition, the estimated temperature niche width of *P. subcurvata* (-2°C – 12.19°C) is wider than that of *P. antarctica* (-2.0°C to 9.52°C) (Table 2); calculated minimum temperatures estimated from the thermal niche width equation were less than -2.0°, the freezing point of seawater, and so growth is assumed to terminate at -2.0°. The Q10 value of the growth rate of *P. antarctica* from 0°C to 4°C is 2.11, which is lower than the Q10 values 3.17 for *P. subcurvata* over the same temperature interval ($p < 0.05$) (Table 2).

3.2 Temperature effects on elemental composition

The C: N and N: P ratios of *P. subcurvata* were unaffected by changing temperature (Fig. 2A, B), but the C: P, C: Si, and C: Chl *a* ratios of this species were significantly affected ($p < 0.05$) (Fig. 2C, D, Fig. 3). The C: P ratios of *P. subcurvata* were slightly but significantly lower in the middle of the tested temperature range. They were higher at 8°C and 10°C than at 2°C, 4°C, and 6°C ($p < 0.05$) (Fig. 2C), and also significantly higher at 10°C than at 0°C (Fig. 2C). The C: Si ratios of *P. subcurvata* showed a similar pattern of slightly lower values at mid-range temperatures; at 0°C and 2°C they were significantly higher than at 6°C and 8°C ($p < 0.05$) (Fig. 2D), and significantly higher at 2°C and 10°C than at 4°C and 8°C, respectively (Fig. 2D). The C: Chl *a* ratios of *P. subcurvata* also showed this trend of somewhat lower values in the middle

of the thermal gradient. At 0°C, 8°C and 10°C, C: Chl *a* ratios were significantly higher than at 2°C, 4°C, and 6°C ($p < 0.05$), and also significantly higher at 10°C than at 0°C and 8°C (Fig. 3).

The C: N, N: P, C: P, and C: Chl *a* ratios of *P. antarctica* were not significantly different across the temperature range (Fig. 2A, B, C, Fig. 3). The N: P ratios of *P. antarctica* were significantly higher than those of *P. subcurvata* at 2°C, 6°C, and 8°C ($p < 0.05$) (Fig. 2B). Additionally, the C: P ratios of *P. antarctica* were significantly higher than those of *P. subcurvata* at 6°C and 8°C ($p < 0.05$) (Fig. 2C), and the C: Chl *a* ratios of *P. antarctica* were significantly higher than values of *P. subcurvata* at all the temperatures tested ($p < 0.05$) (Fig. 3).

Temperature change significantly affected the cellular carbon (C) quotas, cellular nitrogen (N) quotas, cellular phosphorus (P) quotas, cellular silica (Si) quotas, and cellular Chl *a* quotas of *P. subcurvata* ($p < 0.05$) (Table 3). The cellular C and N quotas of *P. subcurvata* were significantly higher at 8°C than at 0°C ($p < 0.05$) (Table 3), the cellular P quotas of *P. subcurvata* were significantly higher at 4°C than at 0°C, 2°C, and 10°C ($p < 0.05$) (Table 3), and the cellular Si quotas of *P. subcurvata* were significantly higher at 8°C than at 0°C and 2°C. Si quotas were also significantly higher at 4°C and 6°C than at 0°C ($p < 0.05$) (Table 3). The extreme temperatures significantly decreased the cellular Chl *a* quotas of *P. subcurvata*, as the cellular Chl *a* quotas of this species were significantly higher at 4°C, 6°C, and 8°C than at 0°C and 10°C ($p < 0.05$) (Table 3).

Temperature change significantly affected the cellular P quotas and cellular Chl *a* quotas of *P. antarctica* ($p < 0.05$), but not the cellular C and N quotas ($p > 0.05$) (Table 3). The cellular P quotas of *P. antarctica* were significantly higher at 0°C than at 8°C ($p < 0.05$) (Table 3), and the Chl *a* quotas of the prymnesiophyte were significantly lower at 8°C than at 0°C, 2°C, and 6°C ($p < 0.05$) (Table 3).

3.3 Co-incubation at two temperatures

A warmer temperature favored the dominance of *P.subcurvata* over *P. antarctica* in the model community experiment. Although *P. subcurvata* increased its abundance relative to the

prymnesiophyte at both temperatures by day 6, this increase was larger and happened much faster at 6°C (from 31% to 72%) relative to 0°C (from 31% to 38%) ($p < 0.05$) (Fig. 4).

3.4 CO_2 effects on specific growth rates at two temperatures

The carbonate system was relatively stable across the range of CO_2 levels during the course of the experiment (Table 1). CO_2 concentration significantly affected the growth rates of *P. subcurvata* at both temperatures (Fig. 5). The growth rates of the diatom at 2°C increased steadily with CO_2 concentration increase from 205 ppm to 425 ppm ($p < 0.05$), but were saturated at 755 ppm and 1730 ppm (Fig. 5A). Similarly, the growth rates of *P. subcurvata* at 8°C increased with CO_2 concentration increase from 205 ppm to 260 ppm ($p < 0.05$), and were saturated at 425 ppm, 755 ppm and 1730 ppm (Fig. 5B). The growth rates of the diatom at all CO_2 concentrations tested at 8°C were significantly higher than at 2°C ($p < 0.05$); for instance, the maximum growth rate of *P. subcurvata* at 8°C was 0.88 d^{-1}, significantly higher than the value of 0.60 d^{-1} at 2°C ($p < 0.0.5$) (Table 4). In addition, the pCO_2 half saturation constant (K_m) of *P. subcurvata* at 8°C was 10.7 ppm, significantly lower than 66.0 ppm at 2°C ($p < 0.0.5$) (Table 4). Thus, temperature and CO_2 concentration increase interactively increased the growth rates of *P. subcurvata* ($p < 0.05$).

CO_2 concentration also significantly affected the growth rates of *P. antarctica* at both 2°C and 8°C. The growth rates of the prymnesiophyte at both 2°C and 8°C increased with CO_2 concentration increase from 100 ppm to 260 ppm ($p < 0.05$), and were saturated at 425 ppm and 755 ppm (Fig. 5C, D). The growth rates of *P. antarctica* at 2°C decreased slightly at 1730 ppm relative to 425 ppm and 755 ppm ($p < 0.05$) (Fig. 5C). The maximum growth rate of *P. antarctica* at 8°C was 0.43 d^{-1}, significantly lower than the value of 0.61 d^{-1} at 2°C ($p < 0.05$) (Table 4). The pCO_2 half saturation constants of *P. antarctica* at 2°C and 8°C were not significantly different (Table 4), and thus no interactive effect of temperature and CO_2 was observed on the growth rate of the prymnesiophyte ($p > 0.05$).

3.5 CO_2 effects on elemental composition at two temperatures

CO_2 concentration variation didn't affect the C: N, N: P, or C: P ratios of *P. subcurvata* at either 2°C or 8°C. The C: Si ratios of *P. subcurvata* were significantly higher at 1730 ppm relative to lower pCO_2 levels, except at 755 ppm at 8°C ($p < 0.05$) (Table 5). The N: P ratios of *P. subcurvata* at 8°C were significantly higher than at 2°C at all the CO_2 levels tested except 100 ppm ($p < 0.05$) (Table 5). The C: P ratios of *P. subcurvata* at 8°C were significantly higher than at 2°C at all the CO_2 levels tested ($p < 0.05$) (Table 5). The C: Si ratios of *P. subcurvata* at CO_2 levels lower than 755 ppm at 8°C were significantly lower than at 2°C ($p < 0.05$) (Table 5). The higher temperature also significantly increased the C: Chl *a* ratios of *P. subcurvata* at all the CO_2 levels tested ($p < 0.05$) (Table 5). Additionally, the temperature increase and CO_2 concentration increase interactively decreased the C: Chl *a* ratios of *P. subcurvata* ($p < 0.05$) (Table 5).

The CO_2 concentration increase did not affect the C: N, N: P, and C: P ratios of *P. antarctica* at either 2°C or 8°C. The carbon to Chl *a* ratios of *P. antarctica* were significantly higher at 1730 ppm than at all lower CO_2 concentrations at 2°C. Similarly, at 8°C the carbon to Chl *a* ratios of this species also were significantly higher at 425 ppm, 755 ppm, and 1730 ppm than at lower CO_2 concentrations ($p < 0.05$) (Table 5), and significantly higher at 1730 ppm than at 425 ppm and 755 ppm ($p < 0.05$) (Table 5).

The warmer temperature significantly decreased the C: N ratios of *P. antarctica* at 260 ppm and 755 ppm CO_2 ($p < 0.05$) (Table 5), and C: P ratios also decreased at 100 ppm and 205 ppm($p < 0.05$) (Table 5). The C: Chl *a* ratios of *P. antarctica* at CO_2 levels higher than 205 ppm were significantly higher at 8°C relative to 2°C ($p < 0.05$) (Table 5). Temperature and CO_2 concentration increase interactively increased the C: Chl *a* ratios of *P. antarctica* ($p < 0.05$) (Table 5).

The CO_2 concentration increase didn't affect the cellular C, N, P, or Si quotas of *P. subcurvata* at 2°C, or the C quotas and N quotas at 8°C. The Si quotas of *P. subcurvata* were significantly lower at 1730 ppm CO_2 than at 100 ppm and 205 ppm at 8°C ($p < 0.05$) (Table 6). The cellular Chl *a* quotas of *P. subcurvata* were significantly lower at 8°C relative to 2°C at CO_2 higher than 205 ppm ($p < 0.05$) (Table 6). The temperature increase significantly increased the

297 cellular Si quota of *P. subcurvata* at all the CO_2 levels tested except 1730 ppm ($p < 0.05$) (Table
298 6). Additionally, warming and CO_2 concentration interactively decreased the cellular Si quotas of
299 *P. subcurvata* ($p < 0.05$) (Table 6).

300 The C, N, and P quotas of *P. antarctica* were not affected by CO_2 increase at 2°C, and N
301 and P quotas were not affected by CO_2 increase at 8°C, either. However, the C quota of *P.*
302 *antarctica* at 1730 ppm CO_2 was significantly higher than CO_2 levels lower than 755 ppm at 8°C
303 ($p < 0.05$) (Table 6). The Chl *a* per cell of *P. antarctica* at 1730 ppm CO_2 was significantly less
304 than at lower CO_2 levels at both 2°C and 8°C ($p < 0.05$) (Table 6). For *P. antarctica*, the Chl *a*
305 per cell values at 100 ppm, 205 ppm, and 755 ppm CO_2 at 8°C were significantly lower relative
306 to 2°C ($p < 0.05$) (Table 6). Temperature increase and CO_2 concentration increase interactively
307 increased the C and N quotas of *P. antarctica* ($p < 0.05$) (Table 6).

308 **4 Discussion**

309 As has been documented in previous work, the diatom *P. subcurvata* and the
310 prymnesiophyte *P. antarctica* responded differently to warming (Xu et al., 2014; Zhu et al.
311 2016). In the Ross Sea as elsewhere, temperature determines both phytoplankton maximum
312 growth rates (Bissinger et al., 2008) and the upper limit of growth (Smith, 1990) in a species-
313 specific manner. Thermal functional response curves of phytoplankton typically increase in a
314 normally distributed pattern, with growth rates increasing up to the optimum temperature range,
315 and then declining when temperature reaches inhibitory levels (Boyd et al., 2013; Fu et al., 2014;
316 Xu et al., 2014; Hutchins and Fu, 2017). Specific growth rates of *P. subcurvata* reached optimal
317 levels at 8°C, demonstrating that this species grows fastest at temperatures substantially above
318 any temperatures found in the present-day Ross Sea. In contrast, growth rates of *P. antarctica*
319 saturated at 2°C. This suggests that *P. subcurvata* may be a superior competitor over *P.*
320 *antarctica* in any realistically foreseeable warming scenario.

321 Zhu et al. (2016) found that 4°C warming significantly promoted the growth rates of *P.*
322 *subcurvata* but not *P. antarctica*. Xu et al. (2014) found that the growth rates of another strain of
323 *P. antarctica* (CCMP3314) decreased in a multi-variable "year 2100 cluster" condition (6°C, 81

Pa CO_2, 150 μmol photons m^{-2} s^{-1}) relative to the "current condition" (2°C, 39 Pa CO_2, and 50 μmol photons m^{-2} s^{-1}) and the "year 2060 condition" (4°C, 61 Pa CO_2, and 100 μmol photons m^{-2} s^{-1}). In our study, the Q10 value of *P. subcurvata* from 0°C to 4°C was 3.11, nearly 50% higher than the Q10 value of *P. antarctica* across the same temperature range (2.17), and similar to the Q10 values observed for different strains of these two species in Zhu et al. (2016). Such Q10 values that substantially exceed the canonical value of 2 are often observed in polar marine organisms (Clarke et al. 1983, Hutchins and Boyd 2016). Our results showed that the maximal thermal limit of *P. antarctica* was reached at 10°C, as was also observed by Buma et al. (1991), while *P. subcurvata* did not cease to grow until 14°C. Clearly, *P. subcurvata* has a superior tolerance to higher temperature compared to *P. antarctica*.

The co-incubation experiment with *P. subcurvata* and *P. antarctica* at 0°C and 6°C confirmed that the diatom retained its growth advantage at the higher temperature when growing together with *P. antarctica*. Although the growth rates of the *P. subcurvata* and *Phaeocystis* cultures were not significantly different at 0°C in unialgal cultures (Fig. 1), the diatom slightly outcompeted the prymnesiophyte even at this temperature. It is possible that there were other types of competitive interactions not related to temperature when these two phytoplankton were grown together. For instance, the nutrient uptake and utilization strategy of *P. subcurvata* could have provided it with an advantage in the co-incubation. However, the competitive advantage enjoyed by the diatom was clearly largest at the higher temperatures, so thermal effects on competition are still evident from this experiment. Although we do not know what role (if any) competition for resources like nutrients may have played in determining the outcome of this experiment, it did demonstrate clearly that thermal growth response trends in simple model communities are in general consistent with those seen in unialgal cultures. Xu el al. (2014) observed that the diatom *Fragilariopsis cylindrus* was dominant over *P. antarctica* under "year 2060 conditions" (4°C, 61 Pa CO_2, and 100 μmol photons m^{-2} s^{-1}). These experiments support the results of a Ross Sea field survey which suggested that water temperature structured the phytoplankton assemblage (Liu and Smith, 2012), and may shed light on why *P. antarctica* is

often dominant in cooler waters in the springtime, while diatoms often dominate in summer (DiTullio and Smith, 1996; Arrigo et al., 1999; DiTullio et al., 2000; Liu and Smith, 2012).

Besides temperature, mixed layer depth and irradiance also likely play a role in the competition between diatoms and *P. antarctica* (Arrigo et al., 1999; Arrigo et al., 2010, Smith and Jones 2015). Arrigo et al. (1999) observed that *P. antarctica* dominated the southern Ross Sea region with deeper mixed layers, while diatom dominated the regions with shallower mixed layer depths. The niches of these two groups of phytoplankton are difficult to define by either light or by temperature, since shallow surface stratification tends to promote both solar heating and high irradiance, while deep mixing often lowers both light and temperatures. It is worth considering whether these two phytoplankton groups are each best adapted to a different environmental matrix of both variables. This concept of different light/temperature niches for Ross Sea diatoms and *P. antarctica* is worthy of further investigation.

Our experiments used nutrient-replete conditions, which are relevant to most of the Ross Sea HNLC region throughout most of the growing season. However, major nutrients sometimes become depleted late in the season on McMurdo Sound, the origin of our culture isolates, as Fe inputs are somewhat higher in these nearshore waters (Bertrand et al. 2015). Experiments using nutrient-limited phytoplankton frequently find differing responses to CO_2 and temperature compared to those of nutrient-replete cells, including sometimes enhanced effects of these global change factors on elemental ratios (Taucher et al. 2015, Sala et al. 2016). Our experiments under high nutrient, Fe-replete conditions thus are likely to best predict possible biological effects of future high CO_2 and temperature during the first half or more of the Ross Sea growing season.

Temperature change affected the C: P, N: P and C: Si ratios of *P. subcurvata*, due to the combined effects of the different responses of cellular C, P, and Si quotas. The C: P and N:P ratios of *P. subcurvata* increased at the two highest temperatures tested. This might be due to an increase in protein translation efficiency and a corresponding decrease in phosphate-rich ribosomes with warming, which can result in a decreased cellular P requirement per unit of carbon in marine phytoplankton (Toseland et al., 2013). Similarly lowered P quotas at higher

temperatures have been documented in other studies as well (Xu et al., 2014; Boyd et al., 2015; Hutchins and Boyd, 2016). This result suggests that the amount of carbon exported per unit phosphorus by *P. subcurvata* (and perhaps other diatoms) in the Ross Sea may increase as temperature increases in the future (Toseland et al., 2013).

In contrast, the decreasing trend of C: Si ratios in *P. subcurvata* appears to be largely due to higher cellular Si quotas at temperatures at and above 4°C. Although the physiological reason(s) for increased silicification with warming are currently not understood, this trend also may have biogeochemical consequences. This decrease of cellular C: Si ratios at higher temperature may tend to enhance Si export, with the qualification that biogenic Si remineralization rates also increase with temperature (Ragueneau et al. 2000), and thus could potentially offset this trend.

Previous studies have shown that nutrient drawdown by diatoms and *P. antarctica* are different, due to differing elemental ratios of these two groups (Arrigo et al., 1999; Smith et al., 2014a; Xu et al., 2014). Our results generally corresponded to this trend, as the N: P ratios of *P. antarctica* were higher than *P. subcurvata* at 2°C, 6°C and 8°C and C: P ratios of *P. antarctica* were higher than *P. subcurvata* at 6°C and 8°C ($p < 0.05$) (Fig. 2). Although elemental ratios of the prymnesiophyte were largely unaffected by temperature, a predicted increase of diatom and decrease of *P. antarctica* contributions to phytoplankton production caused by warming will likely change nutrient export ratios (Smith et al., 2014a, b). It is possible that N and C export per unit P may decrease with a phytoplankton community shift from *P. antarctica* dominance to diatom dominance (Arrigo et al., 1999; Smith et al., 2014a, b; Xu et al., 2014). However, food web effects may compensate for the effects of temperature on biogeochemical cycles, as diatoms are a preferred food source for zooplankton grazers, compared to *Phaeocystis* (Knox, 1994; Caron et al., 2000; Haberman et al., 2003).

Our results showed that the growth rates of both *P. subcurvata* and *P. antarctica* exhibited moderate limitation by CO_2 levels lower than ~425 ppm at both 2°C and 8°C; this observation is significant, since during the intense Ross Sea summertime phytoplankton bloom

405 pCO_2 can sometimes drop to very low levels (Tagliabue and Arrigo, 2016). However, at CO_2
406 concentrations beyond current atmospheric levels of ~400 ppm, growth rates of *P. subcurvata* or
407 *P. antarctica* were CO_2-saturated. Although a general model prediction suggests that an
408 atmospheric CO_2 increase from current levels to 700 ppm could increase the growth of marine
409 phytoplankton by 40% (Schippers et al., 2004), our results instead correspond to previous studies
410 which showed negligible effects of elevated CO_2 on various groups of phytoplankton (Goldman,
411 1999; Fu et al., 2007; Hutchins and Fu 2017). In particular, Trimborn et al. (2013) found that
412 increasing CO_2 had no effect on growth rates of Southern Ocean isolates of *P. subcurvata* and *P.*
413 *antarctica*. The minimal effects of changing CO_2 levels on many phytoplankton groups have
414 been suggested to be due to efficient carbon concentrating mechanisms (CCMs) that allow them
415 to avoid CO_2 limitation at low pCO_2 levels (Burkhardt et al., 2001; Fu et al., 2007; Tortell et al.,
416 2008). For instance, both *P. subcurvata* and *P. antarctica* have been shown to strongly
417 downregulate activity of the important CCM enzyme carbonic anhydrase as CO_2 increases
418 (Trimborn et al. 2013). Clearly, though, for our two species their CCM activity was not sufficient
419 to completely compensate for carbon limitation at low pCO_2 levels. Although speculative, it is
420 possible that *P. antarctica* could have an ability to subsidize growth at very low CO_2 levels
421 through oxidation of organic carbon from the colony mucilage. Our results also showed that
422 very high CO_2 (1730 ppm) significantly reduced the growth rate of *P. antarctica* relative to 425
423 ppm and 755 ppm at 2°C. This inhibitory effect might be due to the significantly lower pH at
424 1730 ppm (~7.4), which could entail expenditures of additional energy to maintain pH
425 homeostasis within cells. Similar negative effects of high CO_2 have been observed on *P.*
426 *antarctica* in natural communities (Hancock et al. 2017), as well as on a mixed Antarctic
427 microbial assemblage (Davidson et al. 2016).
428 Warming from 2°C to 8°C had a significant interactive effect with CO_2 concentration in
429 *P. subcurvata*, as maximum growth rates were higher and the half saturation constant ($K_{1/2}$) for
430 growth was much lower at the warmer temperature. In contrast, warming decreased the maximal
431 growth rates of *P. antarctica* over the range of CO_2 concentrations tested, and failed to change its

$K_{1/2}$ for growth. The decreased CO_2 $K_{1/2}$ of *P. subcurvata* at high temperature might confer a future additional competitive advantage over *P. antarctica* in the late growing season when pCO_2 can be low (Tagliabue and Arrigo, 2016) and temperatures higher, although temperatures are generally never as high as 8°C in the current Ross Sea (Liu and Smith, 2012). The interactive effects of temperature and CO_2 on *P. subcurvata* might be due to elevated enzyme and protein translation efficiencies at higher temperature, which may decrease the CO_2 requirement of the Calvin cycle and facilitate allocation of fixed carbon to growth (Toseland et al., 2013, Hutchins and Boyd 2016). On the other hand, 8°C is clearly close to the upper thermal limit of *P. antarctica*, suggesting that it's biochemical efficiencies decline rapidly above this temperature. The $K_{1/2}$ of *P. antarctica* for CO_2 was however significantly lower than that of *P. subcurvata* at 2°C, which may be advantageous to the prymnesiophyte when water temperatures are low in the spring.

The effects of pCO_2 variation on the elemental ratios of *P. subcurvata* and *P. antarctica* were minimal relative to those of temperature increase. Previous research on the effects of CO_2 on the elemental ratios of phytoplankton has shown that the elemental composition of phytoplankton may change with CO_2 availability (Burkhardt et al., 1999; Fu et al., 2007, 2008; Tew et al., 2014; reviewed in Hutchins et al., 2009). Hoogstraten et al. (2012) found that CO_2 concentration change didn't change the cellular POC, PON, C: N ratios, or POC to Chl *a* ratios of the temperate species *Phaeocystis globosa*. In contrast, Reinfelder (2014) observed that the N and P quotas of several diatoms decreased with increasing CO_2 and led to increased C: N, N: P, and C: P ratios. King et al. (2015) found that high CO_2 could increase, decrease or not affect the C: P and N: P ratios of several different phytoplankton species. Our results resemble those of studies with other phytoplankton that found that the effects of CO_2 concentration can be negligible on C: N, N: P, or C: P ratios (Fu et al., 2007; Hutchins et al., 2009; Hoogstraten et al., 2012; King et al., 2015), including incubation studies with Antarctic communities (Deppeler et al., 2017). It is possible that such contrasting effects of CO_2 concentration on the elemental ratios of phytoplankton are due to species-specific differences in biochemical composition (e.g.,

459 proteins are enriched with N and membranes with P relative to other cellular components), or to
460 differences in experimental design, which can make inter-comparisons problematic (Hutchins
461 and Fu 2017).

462 In contrast to C: N: P ratios, we observed that the C: Si ratios of *P. subcurvata* were
463 significantly higher at 1730 ppm compared to almost all of the lower CO_2 levels. This increase in
464 C: Si ratios was due to a decrease in cellular Si quotas at 1730 ppm CO_2. Milligan et al. (2004)
465 observed that the silica dissolution rates of a temperate diatom increased significantly in high
466 CO_2 relative to in low CO_2 cultures. Tatters et al. (2012) found a similar trend in the temperate
467 toxic diatom *Pseudo-nitzschia fraudulenta*, in which cellular C: Si ratios were higher at 765 ppm
468 than at 200 ppm CO_2. This suggests that future increases in diatom silicification at elevated
469 temperature could partially or wholly offset the decreased silicification and higher dissolution
470 rates of silica observed high CO_2 (above); to fully predict net trends, further interactive
471 experiments focusing on silicification as a function across a range of both temperature and pCO_2
472 are needed.

473 In conclusion, our results indicate that *P. subcurvata* from the Ross Sea are better adapted
474 to higher temperature than is *P. antarctica*. Diatoms are a diverse group, but if their general
475 thermal response is similar to that of this *Pseudo-nitzschia* species, they may thrive under future
476 global warming scenarios while the relative dominance of *P. antarctica* in this region may wane.
477 In contrast, another recent study has suggested that warming might indirectly favor *P. antarctica*
478 springtime dominance by leading to large areas of open water at a time when incident light
479 penetration is low and mixed layers are still relatively deep (Ryan-Keogh et al. 2017). Because
480 of the differences in elemental ratios in the two groups, ecological shifts that favor diatoms may
481 significantly increase the export of phosphorus and silicon relative to carbon and nitrogen, while
482 increased *P. antarctica* dominance will increase carbon export relative to nutrient fluxes, as well
483 as enhancing the organic sulfur cycle. Our conclusions must be qualified as they were obtained
484 using Fe-replete culture conditions, similar to conditions often found early in the growing season
485 in McMurdo Sound. However, Fe limitation generally prevails later in the season here, and

elsewhere in the offshore Ross Sea. Irradiance is an additional key environmental factor to consider in both the present and future in this region (Smith and Jones, 2015). Thus, in addition to warming and CO_2 increases, the interactive effects of light and Fe with these two factors should also be considered (Xu et al., 2014; Boyd et al., 2015; Hutchins and Boyd 2016; Hutchins and Fu 2017). Considering the differences between the responses of the diatom and *P. antarctica* to warming and ocean acidification seen here, as well to warming and Fe in previous work (Zhu et al., 2016), models attempting to predict future changes in community structure and primary production in the Ross Sea polynya may need to realistically incorporate a complex network of interacting global change variables.

Author contribution

Z. Zhu, F. X. Fu, D. A. Hutchins designed the experiments, Z. Zhu, P. Qu, and J. Gale carried them out, and Z. Zhu and D. A. Hutchins wrote the manuscripts.

Competing interests

The authors declare that they have no conflict of interest.

Acknowledgments

We want to thank Kai Xu for isolating all these phytoplankton strains. Support for this research was provided by National Science Foundation grant ANT 1043748 to D. A. Hutchins.

References

Arrigo, K. R., Robinson, D. H., Worthen, D. L., Dunbar, R. B., DiTullio, G. R., VanWoert, M., and Lizotte, M. P.: Phytoplankton community structure and the drawdown of nutrients and CO_2 in the Southern Ocean, Science, 283, 365-367, 1999.

Arrigo K. R., DiTullio G. R., Dunbar R. B., Robinson D. H., Van Woert M., Worthen D. L., Lizotte M. P.: Phytoplankton taxonomic variability in nutrient utilization and primary production in the Ross Sea, J. Geophys Res: Oceans, 105, 8827-8846, 2000.

Arrigo, K. R., van Dijken, G. L., and Bushinsky, S.: Primary production in the Southern Ocean, 1997–2006, J. Geophys Res, 113, C08004, doi:10.1029/2007JC004551, 2008.

Arrigo, K. R., Mills, M. M., Kropuenske, L. R., van Dijken, G. L., Alderkamp, A. C., and Robinson, D. H.: Photophysiology in two major Southern Ocean phytoplankton taxa: photosynthesis and growth of *Phaeocystis antarctica* and *Fragilariopsis cylindrus* under different irradiance levels, Integrative and Comparative Biology, 50(6), 950-966, 2010.

Bertrand, E.M., McCrow, J.P., Zheng, H., Moustafa, A., McQuaid, J., Delmont, T., Post, A., Sipler, R., Spackeen, J., Xu, K., Bronk, D., Hutchins, D.A., and Allen, A.E.: Phytoplankton-bacterial interactions mediate micronutrient colimitation in the Southern Ocean, P. Natl. Acad. Sci. USA, 112. doi:10.1073/pnas.1501615112, 2015.

Bissinger, J. E., Montagnes, D. J., Sharples, J., and Atkinson, D.: Predicting marine phytoplankton maximum growth rates from temperature: Improving on the Eppley curve using quantile regression, Limnol. Oceanogr., 53, 487, 2008.

Boyd, P. W., Rynearson, T. A., Armstrong, E. A., Fu, F., Hayashi, K., Hu, Z., Hutchins, D.A., Kudela, R.M., Litchman, E., Mulholland, M.R. and Passow, U.: Marine phytoplankton temperature versus growth responses from polar to tropical waters–outcome of a scientific community-wide study, PLoS One, 8, available at: http://dx.doi.org/10.1371/journal.pone.0063091, 2013.

Boyd, P. W., Dillingham, P. W., McGraw, C. M., Armstrong, E. A., Cornwall, C. E., Feng, Y. Y., Hurd, C.L., Gault-Ringold, M., Roleda, M.Y., Timmins-Schiffman, E. and Nunn, B. L.: Physiological responses of a Southern Ocean diatom to complex future ocean conditions, Nature Climate Change, 6, 207-213, 2015.

Boyd, P. W., Watson, A. J., Law, C. S., Abraham, E. R., Trull, T., Murdoch, R., Bakker, D. C., Bowie, A. R., Buesseler, K. O., Chang, H., and Charette, M.: A mesoscale phytoplankton bloom in the polar Southern Ocean stimulated by iron fertilization, Nature, 407(6805): 695-702, 2000.

Buma, A. G. J., Bano, N., Veldhuis, M. J. W., and Kraay, G. W.: Comparison of the pigmentation of two strains of the prymnesiophyte *Phaeocystis* sp., Neth. J. Sea Res., 27(2), 173-182, 1991.

539 Burkhardt, S., Zondervan, I., and Riebesell, U.: Effect of CO_2 concentration on C: N: P ratio in
540 marine phytoplankton: A species comparison, Limnol. Oceanogr., 44, 683-690, 1999.
541 Burkhardt, S., Amoroso, G., Riebesell, U., and Sültemeyer, D.: CO_2 and HCO_3^{-1} uptake in
542 marine diatoms acclimated to different CO_2 concentrations, Limnol. Oceanogr., 46, 1378-1391,
543 2001.
544 Caron, D. A., Dennett, M. R., Lonsdale, D. J., Moran, D. M., and Shalapyonok, L.:
545 Microzooplankton herbivory in the Ross sea, Antarctica, Deep-Sea Res. Pt. II, 47(15), 3249-
546 3272, 2000.
547 Chaui-Berlinck, J. G., Monteiro, L. H. A., Navas, C. A., and Bicudo, J. E. P.: Temperature
548 effects on energy metabolism: a dynamic system analysis, P. Roy. Soc. Lond. B Bio., 269, 15-19,
549 2002.
550 Clarke, A. Life in cold water: the physiological ecology of polar marine ectotherms. Oceanogr.
551 Mar Biol. Annu. Rev. 21**:** 341–453, 1983.
552 Coale, K. H., Johnson, K. S., Chavez, F. P., Buesseler, K. O., Barber, R. T., Brzezinski, M. A.,
553 Cochlan, W. P., Millero, F. J., Falkowski, P. G., Bauer, J. E., and Wanninkhof, R. H.: Southern
554 Ocean iron enrichment experiment: carbon cycling in high-and low-Si waters, Science,
555 304(5669), 408-414, 2004.
556 Davidson, A. T., McKinlay, J., Westwood, K., Thompson, P. G., van den Enden, R., de Salas,
557 M., Wright, S., Johnson, R., and Berry, K.: Enhanced CO_2 concentrations change the structure of
558 Antarctic marine microbial communities, Mar. Ecol-Prog. Ser., 552, 92-113, 2016.
559 Deppeler, S., Petrou, K., Schulz, G. K., Westwood K., Pearce, I., McKinlay J., and Davidson A..
560 Ocean acidification of a coastal Antarctic marine microbial community reveals a critical
561 threshold for CO_2 tolerance in phytoplankton productivity. Biogeosciences Discussions,
562 doi.org/10.5194/bg-2017-226, in review, 2017.
563 DiTullio, G. R., and Smith, W. O.: Spatial patterns in phytoplankton biomass and pigment
564 distributions in the Ross Sea. J. Geophys Res: Oceans, 101, 18467-18477, 1996.

565 DiTullio, G. R., Grebmeier, J. M., Arrigo, K. R., Lizotte, M. P., Robinson, D. H., Leventer, A.,
566 Barry, J.P., VanWoert, M.L. and Dunbar, R. B.: Rapid and early export of *Phaeocystis*
567 *antarctica* blooms in the Ross Sea, Antarctica, Nature, 404, 595-598, 2000.
568 El-Sabaawi, R., and Harrison, P. J.: Interactive effects of irradiance and temperature on the
569 photosynthetic physiology of the pennate diatom *Pseudo-nitzschia Granii* (Bacillariophyceae)
570 from the northeast Subarctic Pacific, J. Phycol., 42, 778-785, 2006.
571 Fabry, V. J. (2008). Marine calcifiers in a high-CO_2 ocean. *Science*, 320(5879), 1020-1022.
572 Fu, F. X., Warner, M. E., Zhang, Y., Feng, Y., and Hutchins, D. A.: Effects of increased
573 temperature and CO_2 on photosynthesis, growth, and elemental ratios in marine *Synechococcus*
574 and *Prochlorococcus* (cyanobacteria), J. Phycol., 43, 485-496, 2007.
575 Fu, F. X., Zhang, Y., Warner, M. E., Feng, Y., Sun, J., and Hutchins, D. A.: A comparison of
576 future increased CO_2 and temperature effects on sympatric *Heterosigma akashiwo* and
577 *Prorocentrum minimum*, Harmful Algae, 7, 76-90, 2008.
578 Fu, F. X., Yu, E., Garcia, N. S., Gale, J., Luo, Y., Webb, E. A., and Hutchins, D. A.: Differing
579 responses of marine N_2 fixers to warming and consequences for future diazotroph community
580 structure, Aquat. Microb. Ecol., 72, 33-46, 2014.
581 Gille, S. T.: Warming of the Southern Ocean since the 1950s, Science, 295, 1275-1277, 2002.
582 Goldman, J. C.: Inorganic carbon availability and the growth of large marine diatoms, Mar. Ecol-
583 Prog. Ser., 180, 81-91, 1999.
584 Haberman, K. L., Ross, R. M., and Quetin, L. B.: Diet of the Antarctic krill (Euphausia superba
585 Dana): II. Selective grazing in mixed phytoplankton assemblages, J. Exper. Mar. Biol.
586 Ecol., 283, 97-113, 2003.
587 Hancock, A. M., Davidson, A. T., McKinlay, J., McMinn, A., Schulz, K., and van den Enden, R.
588 L. Ocean acidification changes the structure of an Antarctic coastal protistan community,
589 Biogeosciences Discussions, doi.org/10.5194/bg-2017-224, in review, 2017.

Hoogstraten, A., Peters, M., Timmermans, K. R., and De Baar, H. J. W.: Combined effects of inorganic carbon and light on *Phaeocystis globosa* Scherffel (Prymnesiophyceae), Biogeosciences, 9, 1885-1896, 2012.

Hutchins, D.A., Mulholland, M.R. and Fu, F. X.: Nutrient cycles and marine microbes in a CO_2-enriched ocean, Oceanography, 22, 128-145, 2009.

Hutchins, D.A. and Boyd, P.W.: Marine phytoplankton and the changing ocean iron cycle, Nature Climate Change, 6, 1071-1079, 2016.

Hutchins, D. A., and Fu, F. X.: Microorganisms and ocean global change. *Nature Microbiology*, 2, 17508, doi:10.1038/nmicrobiol.2017.582017.

Hutchins, D. A., Sedwick, P. N., DiTullio, G. R., Boyd, P. W., Queguiner, B., Griffiths, F. B., and Crossley, C.: Control of phytoplankton growth by iron and silicic acid availability in the subantarctic Southern Ocean: Experimental results from the SAZ Project, J. Geophys. Res. Oceans, 106(C12), 31559-31572, 2001.

IPCC, 2014: Climate Change 2014: Impacts, Adaptation, and Vulnerability. Part A: Global and Sectoral Aspects. Contribution of Working Group II to the Fifth Assessment Report of the Intergovernmental Panel on Climate Change.

King, A. L., Sanudo-Wilhelmy, S. A., Leblanc, K., Hutchins, D. A., and Fu, F. X.: CO_2 and vitamin B12 interactions determine bioactive trace metal requirements of a subarctic Pacific diatom, The ISME J., 5, 1388-1396, 2011.

King, A. L., Jenkins, B. D., Wallace, J. R., Liu, Y., Wikfors, G. H., Milke, L. M., and Meseck, S. L.: Effects of CO_2 on growth rate, C: N: P, and fatty acid composition of seven marine phytoplankton species, Mar. Ecol-Prog. Ser., 537, 59-69, 2015.

Knox, G. A.: The Biology of the Southern Ocean, Cambridge University Press, New York, USA, 1994.

Liu, X., and Smith, W. O.: Physiochemical controls on phytoplankton distributions in the Ross Sea, Antarctica, J. Marine Syst., 94, 135-144, 2012.

Martin, J. H., Gordon, R. M., and Fitzwater, S. E.: Iron in Antarctic waters, Nature, 345(6271), 156-158, 1990.

Meredith, M. P., and King, J. C.: Rapid climate change in the ocean west of the Antarctic Peninsula during the second half of the 20th century, Geophys. Res. Lett., 32, L19604, doi:10.1029/2005GL024042, 2005.

Milligan, A. J., Varela, D. E., Brzezinski, M. A., and Morel, F. M.: Dynamics of silicon metabolism and silicon isotopic discrimination in a marine diatom as a function of pCO_2, Limnol. Oceanogr, 49, 322-329, 2004.

Orr, J. C., Fabry, V. J., Aumont, O., Bopp, L., Doney, S. C., Feely, R. A., Gnanadesikan, A., Gruber, N., Ishida, A., Joos, F. and Key, R. M.: Anthropogenic ocean acidification over the twenty-first century and its impact on calcifying organisms, Nature, 437, 681-686, 2005.

Paasche, E.: Silicon and the ecology of marine plankton diatoms. II. Silicate-uptake kinetics in five diatom species, Mar. Biol., 19, 262-269, 1973.

Ragueneau, O., Tréguer, P., Leynaert, A., Anderson, R. F., Brzezinski, M. A., DeMaster, D. J., Fischer, G., Francois, R., and Heinze, C.: A review of the Si cycle in the modern ocean: recent progress and missing gaps in the application of biogenic opal as a paleoproductivity proxy, Global and Planet. Change, 26, 317-365, 2000.

Reinfelder, J. R.: Carbon dioxide regulation of nitrogen and phosphorus in four species of marine phytoplankton, Mar. Ecol-Prog. Ser., 466, 57-67, 2012.

Pierrot, D., Lewis, E., and Wallace, D. W. R.: MS Excel program developed for CO_2 system calculations. ORNL/CDIAC-105a. Carbon Dioxide Information Analysis Center, Oak Ridge National Laboratory, US Department of Energy, Oak Ridge, Tennessee, 2006.

Rose, J. M., Feng, Y., DiTullio, G. R., Dunbar, R. B., Hare, C. E., Lee, P. A., Lohan, M.C., Long, M.C., Smith, W.O., Sohst, B.M., and Tozzi, S.: Synergistic effects of iron and temperature on Antarctic phytoplankton and microzooplankton assemblages, Biogeosciences, 6, 3131-3147, 2009.

642 Ryan-Keogh, T. J., DeLizo, L. M., Smith, W. O. Jr., Smith, Sedwick, P. N., McGillicuddy, D. J.,
643 Jr., Moore, C. M., and Bibby, T. S. Temporal progression of photosynthetic-strategy in
644 phytoplankton in the Ross Sea, Antarctica, J. Mar. Sys., 166, 87-96,
645 DOI:10.1016/j.jmarsys.2016.08.014, 2017.
646 Sala, M. M., Aparicio, F. L., Balague, V., Boras, J. A., Borrull, E., Cardelus, C., Cros,
647 L., Gomes, A., Lopez-Sanz, A., Malits, A., Martinez, R. A., Mestre, M., Movilla, J., Sarmento,
648 H., Vazquez-Dominguez, E., Vaque, D., Pinhassi, J., Calbet, A., Calvo, E., Gasol, J.
649 M., Pelejero, C., Marrase, C. Contrasting effects of ocean acidification on the microbial food
650 web under different trophic conditions. ICES Journal of Marine Science 73(3): 670-679, 2016.
651 Sarmiento, J. L., Hughes, T. M., Stouffer, R. J., and Manabe, S.: Simulated response of the ocean
652 carbon cycle to anthropogenic climate warming, Nature, 393, 245-249, 1998.
653 Schippers, P., Lürling, M., and Scheffer, M.: Increase of atmospheric CO_2 promotes
654 phytoplankton productivity, Ecol. Lett, 7, 446-451, 2004.
655 Schoemann V., Becquevort S., Stefels J., Rousseau V., Lancelot C.: *Phaeocystis* blooms in the
656 global ocean and their controlling mechanisms: a review, J. Sea Res., 53, 43-66, 2005.
657 In: Smith, W. O.: Polar Oceanography, Chemistry, Biology and Geology, Academic Press,
658 Massachusetts, USA, 1990.
659 Sedwick, P. N., DiTullio, G. R., and Mackey, D. J.: Iron and manganese in the Ross Sea,
660 Antarctica: Seasonal iron limitation in Antarctic shelf waters, J. Geophys. Res.: Oceans,
661 105(C5), 11321-11336, 2000.
662 Sedwick, P. N., Marsay, C. M., Sohst, B. M., Aguilar-Islas, A. M., Lohan, M. C., Long, M. C.,
663 Arrigo, K. R., Dunbar, R. B., Saito, M. A., Smith, W. O., and DiTullio, G. R.: Early season
664 depletion of dissolved iron in the Ross Sea polynya: Implications for iron dynamics on the
665 Antarctic continental shelf. J. Geophys. Res.: Oceans, 116: C12019, DOI:
666 10.1029/2010JC006553, 2011.
667 Smith, W. O., Ainley, D. G., Arrigo, K. R., and Dinniman, M. S.: The oceanography and ecology
668 of the Ross Sea. Annual Review of Marine Science, 6, 469-487, 2014a.

669 Smith, W. O., Dinniman, M. S., Hofmann, E. E., and Klinck, J. M.: The effects of changing
670 winds and temperatures on the oceanography of the Ross Sea in the 21st century. GeophyS. Res.
671 Lett., 41, 1624-1631, 2014b.
672 Smith, W.O., Jr., and Jones, R.M.: Vertical mixing, critical depths, and phytoplankton growth in
673 the Ross Sea. ICES J. Mar. Sci., 72, 6, 1952-1960, 2015.
674 Smith, W. O., Marra, J., Hiscock, M. R., and Barber, R. T.: The seasonal cycle of phytoplankton
675 biomass and primary productivity in the Ross Sea, Antarctica, Deep-Sea Res. Pt. II, 47, 3119-
676 3140, 2000.
677 Takeda S.: Influence of iron availability on nutrient consumption ratio of diatoms in oceanic
678 waters, Nature, 393(6687), 774-777, 1998.
679 Tagliabue, A., and Arrigo, K.R.: Decadal trends in air-sea CO_2 exchange in the Ross Sea
680 (Antarctica), Geophys. Res. Lett., 43, 5271-5278, 2016.
681 Tatters, A.O., Fu, F.X. and Hutchins, D.A.: High CO_2 and silicate limitation synergistically
682 increase the toxicity of *Pseudo-nitzshia fraudulenta*, PLoS ONE, 7, available at:
683 http://dx.doi.org/10.1371/journal.pone.0032116, 2012.
684 Taucher, J., Jones, J., James, A., Brzezinski, M.A., Carlson, C.A., Riebesell, U., and Passow, U.
685 Combined effects of CO_2 and temperature on carbon uptake and partitioning by the marine
686 diatoms *Thalassiosira weissflogii* and *Dactyliosolen fragilissimus*. Limnol. Oceanogr 60(3): 901-
687 919, 2015.
688 Tew, K. S., Kao, Y. C., Ko, F. C., Kuo, J., Meng, P. J., Liu, P. J., and Glover, D. C.: Effects of
689 elevated CO_2 and temperature on the growth, elemental composition, and cell size of two marine
690 diatoms: potential implications of global climate change, Hydrobiologia, 741, 79-87, 2014.
691 Thomas, M. K., Kremer, C. T., Klausmeier, C. A., and Litchman, E.: A global pattern of thermal
692 adaptation in marine phytoplankton, Science, 338, 1085-1088, 2012.
693 Tortell, P. D., Payne, C., Gueguen, C., Li, Y., Strzepek, R. F., Boyd, P. W., and Rost, B., Uptake
694 and assimilation of inorganic carbon by Southern Ocean phytoplankton. Limnol. Oceanogr., 53,
695 1266-1278, 2008.

Toseland, A. D. S. J., Daines, S. J., Clark, J. R., Kirkham, A., Strauss, J., Uhlig, C., Lenton, T.M., Valentin, K., Pearson, G.A., Moulton, V. and Mock, T. (2013). The impact of temperature on marine phytoplankton resource allocation and metabolism. Nature Climate Change, 3(11), 979-984.

Treguer, P., Nelson, D. M., Van Bennekom, A. J., and DeMaster, D. J.: The silica balance in the world ocean: a reestimate, Science, 268, 375, 1995.

Trimborn, S., Brenneis, T., Sweet, E., and Rost, B.: Sensitivity of Antarctic phytoplankton species to ocean acidification: Growth, carbon acquisition, and species interaction, Limnol. Oceanogr., 58, 997-1007, 2013.

Wang, Y., Smith, W. O., Wang, X., and Li, S.: Subtle biological responses to increased CO_2 concentrations by *Phaeocystis globosa* Scherffel, a harmful algal bloom species, Geophys. Res. Lett., 37, L09604, doi:10.1029/2010GL042666, 2010.

Xu, K., Fu, F. X., and Hutchins, D. A.: Comparative responses of two dominant Antarctic phytoplankton taxa to interactions between ocean acidification, warming, irradiance, and iron availability, Limnol. Oceanogr., 59, 1919-1931, 2014.

Zhu, Z., Xu, K., Fu, F., Spackeen, J. L., Bronk, D. A., and Hutchins, D. A.: A comparative study of iron and temperature interactive effects on diatoms and *Phaeocystis antarctica* from the Ross Sea, Antarctica, Mar. Ecol-Prog. Ser., 550, 39-51, 2016.

715 Table 1. The measured pH and dissolved inorganic carbon (DIC), and calculated pCO_2 of *P. subcurvata*
716 and *P. antarctica* at 2°C and 8°C in each treatment. Values represent the means and errors are the
717 standard deviations of triplicate bottles.

718

P. subcurvata		*P. antarctica*	
2°C	8°C	2°C	8°C
pH			
8.36±0.04	8.51±0.04	8.40±0.03	8.45±0.03
8.25±0.04	8.36±0.01	8.22±0.04	8.29±0.01
8.07±0.01	8.17±0.01	8.09±0.02	8.14±0.00
7.86±0.02	7.99±0.01	7.85±0.01	7.94±0.00
7.68±0.01	7.79±0.02	7.65±0.01	7.75±0.00
7.35±0.01	7.46±0.02	7.34±0.01	7.45±0.00
DIC (µmol/kg)			
1890.1±26.6	1846.5±15.8	1847.1±30.0	1831.1±22.7
2049.1±10.8	1985.7±2.1	2033.9±15.0	2014.2±19.9
2131.3±9.4	2067.5±4.7	2136.6±5.6	2085.3±15.3
2190.4±2.8	2156.1±13.9	2168.1±12.4	2167.4±21.5
2260.0±22.2	2234.8±10.3	2252.1±11.5	2238.7±12.0
2340.1±19.4	2334.5±18.8	2338.2±12.1	2323.7±11.5
pCO_2 (ppm)			
109.1±9.3	94.4±10.1	96.6±9.5	108.8±8.8
158.6±15.5	150.3±3.6	171.2±14.4	183.6±4.2
263.1±5.9	254.2±9.9	246.4±9.9	280.3±0.6
450.2±17.3	414.9±12.0	462.2±12.1	480.9±4.7
740.9±10.6	708.8±23.5	786.9±10.3	784.1±4.8
1751.2±35.9	1675.3±49.4	1769.9±59.5	1720.3±18.3

719
720
721

722 Table 2. Statistical comparison of the results for each of the three thermal traits: Optimum temperature
723 (ºC), Maximum growth rate (d^{-1}) and temperature niche width (W)* of *P. subcurvata* and *P. antarctica.*
724

Species	Optimum temperature (ºC)	Maximum growth rates (d^{-1})	W upper CI	W lower CI	Q_{10}
P. subcurvata	7.36	0.86	12.19	< -2.0	3.17
P. antarctica	4.85	0.66	9.52	< -2.0	2.11

725
726 * The statistical results for the lower bound of temperate niche width in both species were lower
727 than -2.0ºC, the freezing point of seawater
728

729 Table 3. The effects of temperature on the C quota (pmol cell^{-1}), N quota (pmol cell^{-1}), P quota (pmol
730 cell^{-1}), Si quota (pmol cell^{-1}), and chl *a* per cell (pg cell^{-1}) of *P. subcurvata* and *P. antarctica.* Values
731 represent the means and errors are the standard deviations of triplicate bottles.
732

	P. subcurvata	*P. antarctica*
C quota		
0°C	1.91±0.14	2.64±0.34
2°C	2.11±0.19	2.49±0.41
4°C	2.15±0.12	2.50±0.23
6°C	2.07±0.13	2.26±0.18
8°C	2.33±0.14	2.17±0.22
10°C	2.17±0.13	
N quota		
0°C	0.27±0.03	0.39±0.03
2°C	0.29±0.03	0.36±0.02
4°C	0.33±0.02	0.40±0.01
6°C	0.31±0.01	0.35±0.02
8°C	0.36±0.05	0.34±0.03
10°C	0.33±0.04	
P quota		
0°C	0.02±0.00	0.03±0.00
2°C	0.02±0.00	0.02±0.00
4°C	0.03±0.00	0.03±0.01
6°C	0.03±0.00	0.02±0.00
8°C	0.03±0.00	0.02±0.00
10°C	0.02±0.00	
Si quota		
0°C	0.23±0.02	
2°C	0.23±0.06	
4°C	0.30±0.01	
6°C	0.30±0.03	
8°C	0.34±0.01	
10°C	0.28±0.04	
Chl a per cell (pg/cell)		
0°C	0.48±0.01	0.23±0.03
2°C	0.57±0.07	0.22±0.02
4°C	0.64±0.01	0.20±0.01
6°C	0.68±0.05	0.21±0.00
8°C	0.58±0.03	0.17±0.02
10°C	0.46±0.03	

733
734
735

736 Table 4. Comparison of the curve fitting results for maximum growth rate (d^{-1}) and half saturation
737 constants (K_m), calculated from the CO_2 functional response curves of *P. subcurvata* and *P. antarctica* at
738 2°C and 8°C. Values represent the means and errors are the standard errors from fitting.
739 .

Species	Maximum growth rates (d^{-1})	K_m
P. subcurvata		
2°C	0.60±0.18	66.4±10.39
8°C	0.88±0.02	9.8±5.34
P. antarctica		
2°C	0.61±0.02	26.4±8.23
8°C	0.41±0.02	22.1±11.15

740

741 Table 5 The effects of CO_2 on the C: N, N: P, C: P, C: Si, and C: Chl *a* ratios of *P. subcurvata* and *P.*

742 *antarctica* at 2°C and 8°C. Values represent the means and errors are the standard deviations of triplicate

743 bottles.

	P. subcurvata		*P. antarctica*	
	2°C	8°C	2°C	8°C
C: N				
100 ppm	6.6±0.26	7.1±0.68	7.22±0.50	6.95±0.35
205 ppm	6.7±0.24	7.5±0.32	7.74±0.21	6.56±1.15
260 ppm	6.7±0.32	7.3±0.18	8.07±0.52	6.99±0.27
425 ppm	6.7±0.05	6.6±0.05	7.21±0.81	6.19±0.13
755 ppm	6.8±0.20	7.1±0.68	7.98±0.44	6.79±0.22
1730 ppm	7.1±0.82	7.4±1.07	8.15±0.48	7.05±0.91
N: P				
100 ppm	10.4±0.85	14.5±2.28	16.4±1.24	13.9±0.20
205 ppm	10.8±1.01	13.3±0.42	16.6±1.12	15.7±2.77
260 ppm	10.3±1.28	14.0±0.56	14.3±1.24	14.5±2.38
425 ppm	11.3±0.84	16.5±0.28	17.1±1.83	17.2±1.98
755 ppm	9.9±0.28	14.3±1.34	14.2±2.60	11.6±4.11
1730 ppm	10.4±1.02	15.5±1.84	15.5±0.56	15.1±1.85
C: P				
100 ppm	68.6±3.10	101.0±6.43	117.7±4.08	96.7±4.86
205 ppm	72.7±4.82	99.3±7.05	128.2±5.98	101.0±1.91
260 ppm	69.1±7.68	103.0±4.88	115.5±7.25	101.0±13.04
425 ppm	76.3±5.19	109.0±2.20	122.3±4.85	106.0±11.14
755 ppm	67.2±1.38	101.0±5.80	113.5±22.50	78.6±27.09
1730 ppm	73.4±1.22	114.0±5.99	126.2±12.10	105.0±6.26
C: Si				
100 ppm	7.8±0.80	5.6±0.32		
205 ppm	7.4±0.30	5.6±0.24		
260 ppm	7.3±0.23	6.1±0.38		
425 ppm	7.5±0.23	6.1±0.06		
755 ppm	7.4±0.66	6.3±0.36		
1730 ppm	8.0±0.88	7.1±0.47		
C: Chl *a* (µg/µg)				
100 ppm	43.6±1.14	70.7±5.01	160.4±6.68	197.4±29.35
205 ppm	45.2±2.91	67.3±4.42	157.5±4.95	194.0±17.14
260 ppm	41.6±3.31	60.1±9.45	138.3±15.19	169.8±9.20
425 ppm	37.2±2.58	72.5±2.35	180.2±20.10	232.4±20.47
755 ppm	42.2±3.62	68.7±6.29	167.5±5.06	282.5±15.30
1730 ppm	46.3±2.23	85.3±15.70	276.5±36.57	460.3±15.21

744
745
746
747
748
749
750

751 Table 6 The effects of CO_2 on the C quota (pmol cell^{-1}), N quota (pmol cell^{-1}), P quota (pmol cell^{-1}), Si

752 quota (pmol cell^{-1}), and chl *a* per cell (pg cell^{-1}) of *P. subcurvata* and *P. antarctica* at 2°C and 8°C.

753 Values represent the means and errors are the standard deviations of triplicate bottles.

	P. subcurvata		*P. antarctica*	
	2°C	8°C	2°C	8°C
C quota				
100 ppm	2.0±0.15	2.64±0.06	2.57±0.03	2.15±0.22
205 ppm	2.1±0.12	2.67±0.31	2.72±0.28	2.35±0.19
260 ppm	1.9±0.04	2.28±0.18	2.51±0.36	2.21±0.04
425 ppm	1.8±0.04	2.43±0.15	2.31±0.05	2.28±0.46
755 ppm	2.1±0.09	2.26±0.05	2.47±0.17	2.81±0.15
1730 ppm	2.1±0.30	2.47±0.18	2.43±0.10	2.96±0.30
N quota				
100 ppm	0.30±0.03	0.38±0.04	0.36±0.03	0.31±0.03
205 ppm	0.30±0.03	0.36±0.03	0.35±0.03	0.36±0.06
260 ppm	0.29±0.01	0.31±0.02	0.31±0.06	0.32±0.02
425 ppm	0.27±0.01	0.37±0.06	0.32±0.03	0.37±0.05
755 ppm	0.30±0.02	0.32±0.03	0.31±0.03	0.41±0.01
1730 ppm	0.29±0.05	0.34±0.06	0.30±0.03	0.43±0.10
P quota				
100 ppm	0.03±0.00	0.03±0.00	0.02±0.00	0.02±0.00
205 ppm	0.03±0.00	0.03±0.00	0.02±0.00	0.02±0.00
260 ppm	0.03±0.00	0.02±0.00	0.02±0.00	0.02±0.00
425 ppm	0.02±0.00	0.02±0.00	0.02±0.00	0.02±0.01
755 ppm	0.03±0.00	0.02±0.00	0.02±0.00	0.04±0.02
1730 ppm	0.03±0.00	0.02±0.00	0.02±0.00	0.03±0.00
Si quota				
100 ppm	0.26±0.02	0.47±0.04		
205 ppm	0.28±0.02	0.48±0.07		
260 ppm	0.27±0.01	0.37±0.03		
425 ppm	0.25±0.01	0.40±0.04		
755 ppm	0.28±0.03	0.36±0.03		
1730 ppm	0.26±0.01	0.35±0.05		
Chl a per cell (pg/cell)				
100 ppm	0.54±0.05	0.45±0.04	0.19±0.01	0.13±0.02
205 ppm	0.54±0.04	0.48±0.05	0.21±0.02	0.15±0.02
260 ppm	0.56±0.03	0.46±0.04	0.22±0.04	0.16±0.01
425 ppm	0.60±0.04	0.40±0.04	0.16±0.02	0.12±0.01
755 ppm	0.59±0.06	0.40±0.03	0.18±0.01	0.12±0.00
1730 ppm	0.53±0.06	0.35±0.05	0.11±0.02	0.08±0.01

754
755
756

Figure legends

Fig. 1. Thermal functional response curves showing specific growth rates (and fitted curves) of *Pseudo-nitzschia subcurvata* and *Phaeocystis antarctica* across a range of temperatures from 0ºC to 14ºC. Values represent the means and error bars represents the standard deviations of triplicate samples.

Fig. 2. The C: N ratios (A), N: P ratios (B), and C: P ratios (C) of *Pseudo-nitzschia subcurvata* and *Phaeocystis antarctica* and (D) the C: Si ratios of *Pseudo-nitzschia subcurvata* from the thermal response curves shown in Fig. 1 for a range of temperatures from 0ºC to 10ºC. Values represent the means and error bars represents the standard deviations of triplicate samples.

Fig. 3. The C: Chl *a* ratios of *Pseudo-nitzschia subcurvata* and *Phaeocystis antarctica* from the thermal response curves shown in Fig. 1 for a range of temperatures from 0ºC to 10ºC. Values represent the means and error bars represents the standard deviations of triplicate samples.

Fig. 4. The relative abundance of *Pseudo-nitzschia subcurvata* in a 6 day competition experiment with *Phaeocystis antarctica* at 0°C and 6°C. The competition experiments were started with equal Chl *a* concentrations for both species, and the relative abundance was calculated based on cell counts. Values represent the means and error bars represents the standard deviations of triplicate samples.

Fig. 5. CO_2 functional response curves showing specific growth rates (and fitted curves) across a range of CO_2 concentrations from ~100 ppm to ~1730 ppm at 2°C and at 8°C. *Pseudo-nitzschia subcurvata* at 2°C (A) and 8°C (B) and *Phaeocystis antarctica* at 2°C (C) and 8°C (D). Values represent the means and error bars represents the standard deviations of triplicate samples.

786 Fig. 1
787

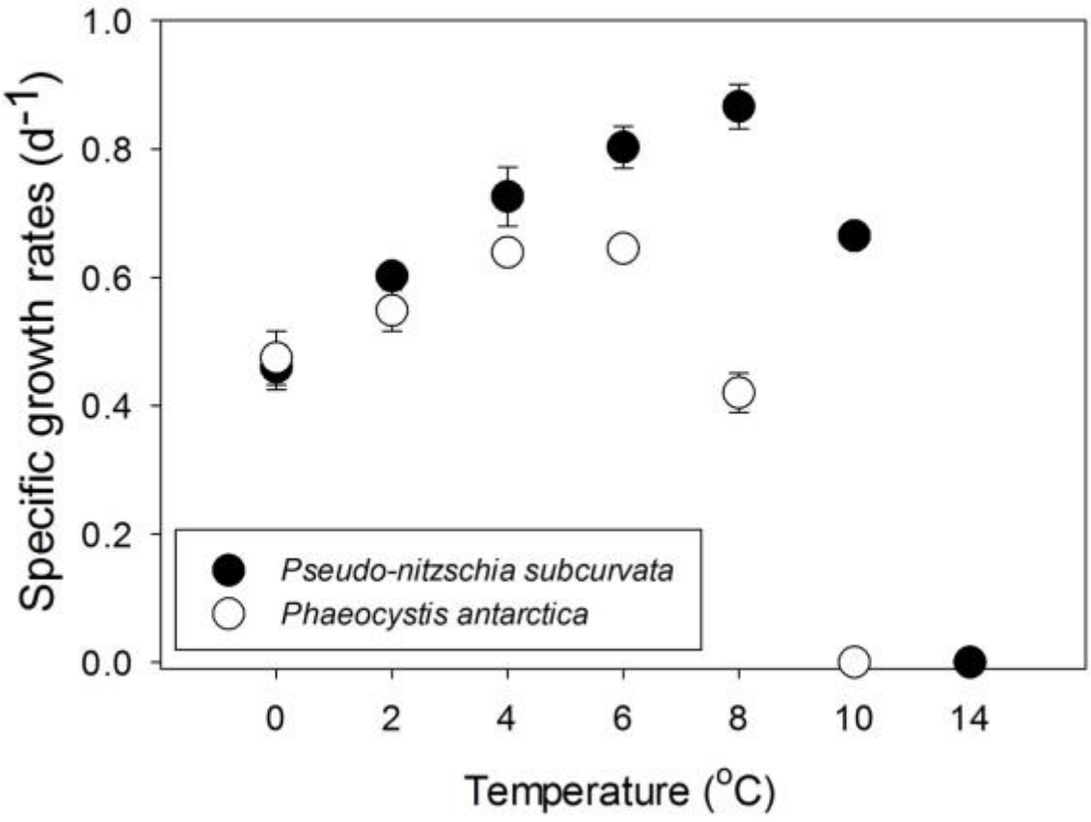
Specific growth rates (d-1)
1.0
0.8
0.6
0.4
0.2
0.0
0
2
4
6
8
10
14
Temperature (°C)
Pseudo-nitzschia subcurvata
Phaeocystis antarctica

Fig. 2

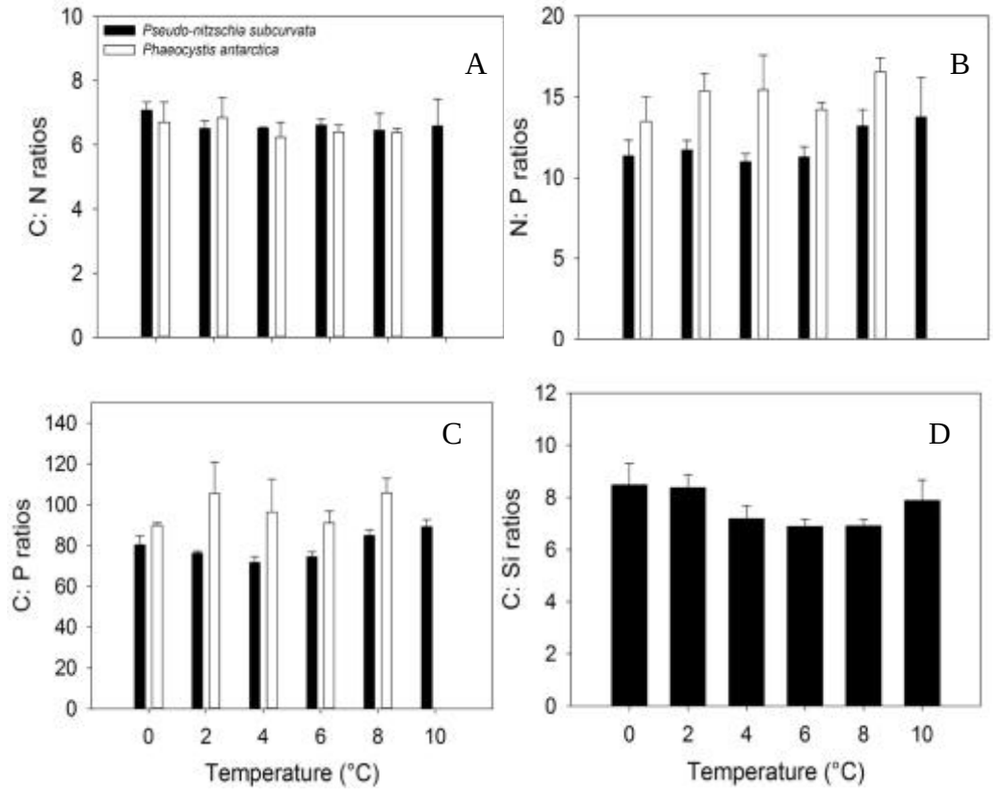
Pseudo-nitzschia subcurvata
Phaeocystis antarctica
A
B
C
D
C: N ratios
N: P ratios
C: P ratios
C: Si ratios
Temperature (°C)
Temperature (°C)

802 Fig. 3

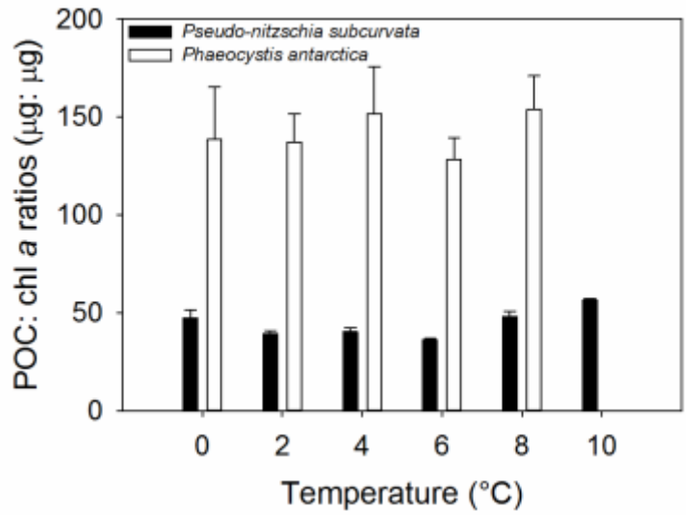
Pseudo-nitzschia subcurvata
Phaeocystis antarctica
POC: chl a ratios (µg: µg)
200
150
100
50
0
0
2
4
6
8
10
Temperature (°C)

803 Fig. 4
804

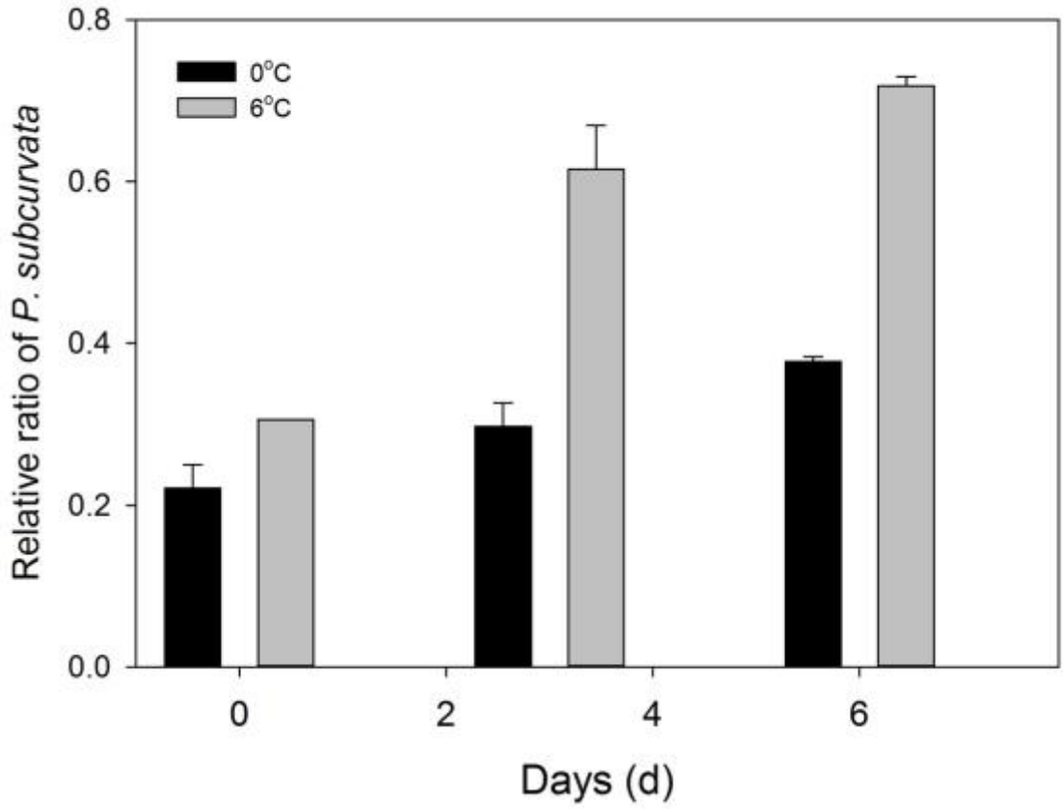

805 Fig. 5

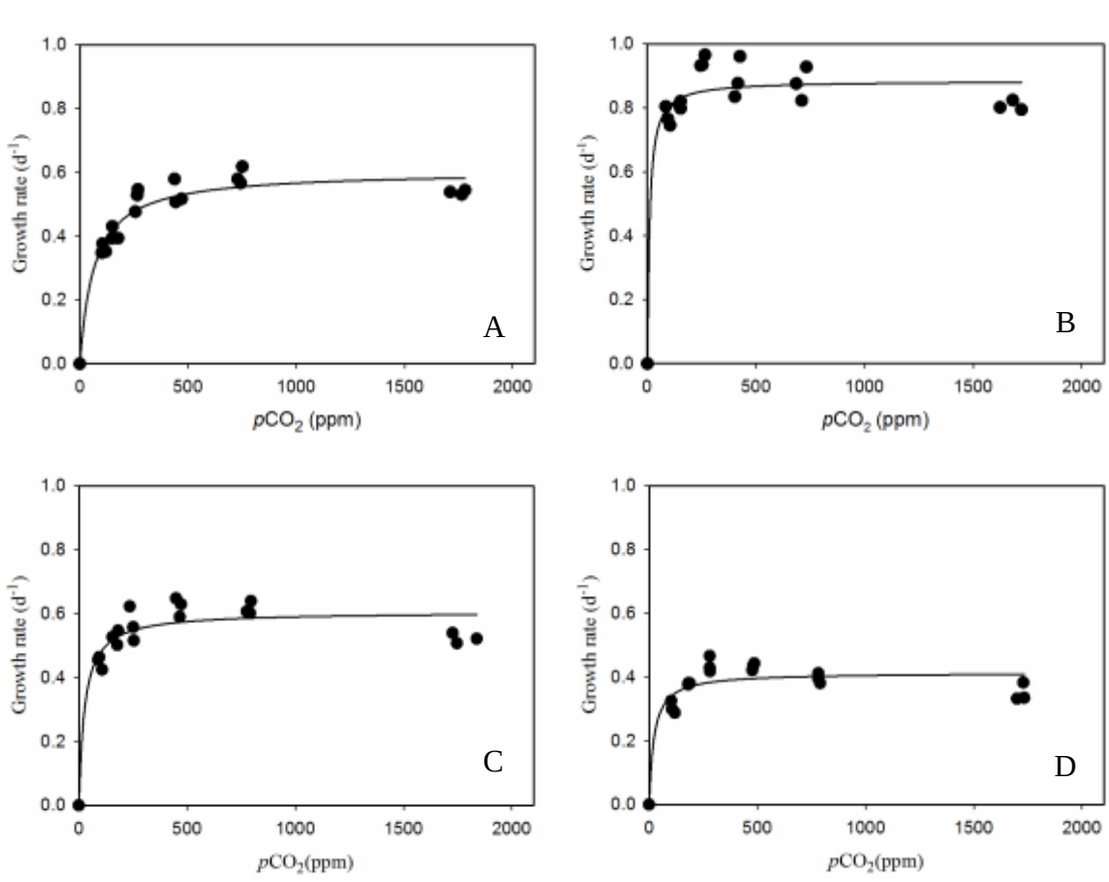
Growth rate (d^{-1})
pCO$_2$ (ppm)
A
B
C
D
0.0
0.2
0.4
0.6
0.8
1.0
0
500
1000
1500
2000